Behav Res
DOI 10.3758/s13428-012-0277-y

Electromagnetic tracking of motion in the proximity of computer generated graphical stimuli: A tutorial

Ulf H. Schnabel · Michael Hegenloh · Hermann J. Müller · Michael Zehetleitner

Abstract Electromagnetic motion-tracking systems have the advantage of capturing the tempo-spatial kinematics of movements independently of the visibility of the sensors. However, they are limited in that they cannot be used in the proximity of electromagnetic field sources, such as computer monitors. This prevents exploiting the tracking potential of the sensor system together with that of computer-generated visual stimulation. Here we present a solution for presenting computer-generated visual stimulation that does not distort the electromagnetic field required for precise motion tracking, by means of a back projection medium. In one experiment, we verify that cathode ray tube monitors, as well as thin-film-transistor monitors, distort electro-magnetic sensor signals even at a distance of 18 cm. Our back projection medium, by contrast, leads to no distortion of the motion-tracking signals even when the sensor is touching the medium. This novel solution permits combining the advantages of electromagnetic motion tracking with computer-generated visual stimulation.

U. H. Schnabel · M. Hegenloh · H. J. Müller · M. Zehetleitner
Ludwig-Maximilians-Universität München,
Munich, Germany

U. H. Schnabel
Neuro-Cognitve Psychology,
München, Germany

M. Hegenloh
Graduate School of Systemic Neurosciences,
Ludwig-Maximilians-Universität München,
Martinsried, Germany

H. J. Müller
Birkbeck College,
London, UK

M. Zehetleitner (✉)
Department of Psychology,
Ludwig-Maximilians-Universität München,
Leopoldstr. 13,
80802 Munich, Germany
e-mail: mzehetleitner@psy.lmu.de

Published online: 13 December 2012

Keywords Electromagnetic motion-tracking · Back projection setup · Measurement accuracy · Experimental setup

Introduction

Movement analysis provides valuable insights into how movements are planned and controlled by the brain (e.g., Körding & Wolpert, 2006; Todorov, 2009), as well as how perception/attention and action are interrelated (e.g., Ernst, 2007; Hommel, 2004; Prinz, 1984, 1997). There exist several methods for recording movement data for analysis, ranging from touchscreens, which can capture only spatial and temporal characteristics of touches and releases, through marker-based camera systems (e.g., OPTOTREK; Northern Digital, Waterloo, Ontario, Canada) and mechanical sensing (e.g., SensAble Technologies Inc., Woburn, MA) to electromagnetic sensors (e.g., Polhemus Inc., Colchester, VT).

When movements were investigated in relation to graphical stimuli, either real objects (e.g., Striemer, Chapman, & Goodale, 2009) or half-transluctant mirror setups (e.g., Baldauf & Deubel, 2008; Diedrichsen, Ivry, Hazeltine, Kennerley, & Cohen, 2003; Ghahramani, Wolpert, & Jordan, 1996; Jonikaitis & Deubel, 2011) were used. Also used were touch screens or tablet PCs with a touch-sensitive layer, which offer easy control of graphical stimulation, although at the cost of measuring only the onsets and offsets of movements—but not their spatio-temporal kinematics (e.g., Basile & Hampton, 2011; Song, Takahashi, & McPeek, 2008; Zehetleitner, Hegenloh, & Müller, 2011).

Presentation of computer-generated graphical stimulation is particularly limited with electromagnetic sensor systems, because the electromagnetic fields of the monitors (e.g., cathode ray tube [CRT] or thin-film-transistor [TFT]) interfere with the sensor signals. Electromagnetic sensor systems, like the Pholemus Liberty (Polhemus Inc., Colchester, VT), work by generating an electromagnetic field with known properties. The sensor registers the electromagnetic field, thus permitting the 3-D position to be computed at each time point, as well as

the tilt and roll of the sensor. Calculation of the 3-D sensor position is predicated on the fact that the electromagnetic field generated by the device is undistorted. When there are additional sources of electromagnetic fields, the reference field is distorted, rendering the calculation of the sensor position invalid. Here, we present a low-priced (~650 Euro) method of presenting computer-generated graphical stimuli that is usable with electromagnetic sensor systems. In short, the method consists of a back projection solution, where a special Plexiglas (polymethyl metacrylate) medium is illuminated from behind using a video projector. For instance, when the back projection medium is mounted in a table surface with the projector placed underneath, it is possible to use full control of computer-generated graphical stimuli, while at the same time the electromagnetic sensor system is unperturbed when the observer is in close proximity to or touching the stimuli.

First, we present empirical data about the distortion of electromagnetic sensor signals depending on the distance to a presentation surface (0–20 cm) and the type of presentation device (CRT, TFT monitor, or our back projection system). Second, we present a tutorial describing the geometric calculations necessary to mount the back projection solution into a table surface.

The goal of the present experiment is to measure signal distortion of an electromagnetic movement measuring system dependent on the proximity to a medium for presenting computer generated graphical stimuli. The aim is to demonstrate that electronic media (CRTs or TFT monitors) distort motion signals, whereas our nonelectronic back projection medium leaves signal quality unaffected by proximity to the medium.

Method

We tested two different monitors: a ViewSonic Graphics Series G90fB CRT (ViewSonic Corporation, Walnut, CA), a DELL E196FP TFT (DELL Inc., Round Rock, TX), as well as our back projection surface. All devices presented a white screen with a luminance of 122 cd/m^2 on the CRT display, 140 cd/m^2 on the TFT display, and 435 cd/m^2 on the back projection surface. In order to test the accuracy of the electromagnetic signals, we placed the sensors at 90 known locations in front of the presentation surface and determined the difference between the measured and real positions dependent on the distance between the sensor and the presentation surface. We chose static positions instead of movements, since measuring static positions is more exact, easier to realize technically, and, most important, a movement measured with magnetic trackers is equivalent to a series of static positions over a series of points in time.

Control of real sensor positions

Real positions were controlled by a wooden frame. The wooden frame contained nine slots arranged in a 3 × 3 matrix into which the sensor could be fitted, resulting in 9 possible positions on the *x*/*y* plane parallel to the presentation surface. Distance orthogonal to the presentation surface (*z*-axis) was controlled by placing the wooden frame at 10 varying distances (0–18 cm in steps of 2 cm) to the surface. At each of the 90 possible positions (9 *x*/*y* positions crossed with 10 *z* positions) of the sensor, 1,000 data points were measured, permitting calculation of the signal variance. The wooden board into which the sensors could be fixed contained nine dents. One dent was located in the center of the board aligned with the center of the presentation surface. Four dents were placed 10 cm to the top, bottom, left, and right of the center (forming a diamond shape). Four further dents were placed on the edges of a square with an edge length of 30 cm (see schematic depiction in Fig. 1).

Setup

We built the setup onto a table in a large room (ca. 5 × 2 m) and removed all metallic objects within a radius of 2 m from the table. To measure the positions in space, we used the Polhemus Liberty motion-tracking system (Polhemus Inc., Colchester, VT) that consists of a base station, a reception cube that projects a magnetic field in the surrounding and small sensors that are connected to the base station. The system allows tracking the position of the sensors in 3-D space at a frequency of 220 Hz. The reception cube of the Polhemus Liberty (Polhemus Inc., Colchester, VT) motion-tracking system was fixed on the table. The vertical surface was located at the same position for all tested presentation media.

Results and discussion

At each of the 90 measured positions, 1,000 measurements were taken. These repeated measurements at the same location were very reliable, with a standard deviation of 0.4 mm. The main independent variable further analyzed was the measurement error—that is, how far the measured position returned by the Polhemus system deviated from the real position (determined by the position of the sensor within the wooden board). The measurement error was calculated as the Euclidian distance between the measured and the real sensor position. Figure 2 presents the measurement error for the TFT and the CRT presentation device (panels a and b, respectively). In each panel, the measurement error of our back projection medium is depicted as well. At each distance from the presentation surface (0–18 cm), the measurement error of all nine points within the *x*/*y* plane are depicted as desaturated points, the mean of which is depicted in saturated colors, for the electromagnetic device (in black color) and the nonelectromagentic device (in green color). As can be seen from Fig. 2a, b, first, the measurement error

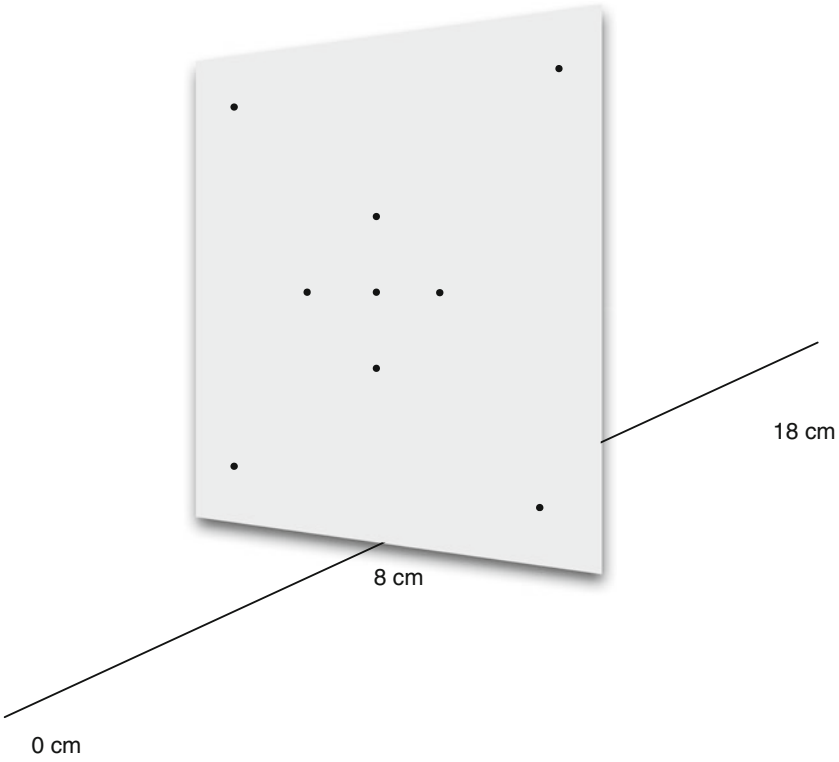

Fig. 1 Real sensor positions were controlled by inserting the sensor into one of nine dents in a wooden board that could be placed at 10 distances from the projection surface. Depicted is a sketch of the situation, where the board was presented at a distance of 8 cm from the projection surface

of the electromagnetic devices increases drastically, the closer the sensor is placed to the presentation medium. Even at the largest distance measured (18 cm), the mean measurement error was ca. 21 cm for both the TFT and CRT monitors, respectively. Measuring directly on the presentation surface leads to mean measurement errors of 20 cm for both TFT and CRT monitors. For the back projection medium, the measurement error is ca. 0.4 cm for each level of distance. Please refer to Tables 1, 2 and 3 in the Appendix for the exact numerical values of measurement error for each measured position and for each device.

Second, at each level of distance from the projection surface, the measurement error varies for different points on the *x*/*y* plane parallel to the surface. For instance, at a distance of 0 cm to the presentation surface, the measurement error varies between 5 and 60 cm for different points on the *x*/*y* plane. This indicates that the distortion generated by the electromagnetic monitors is not homogeneous within a plane parallel to the projection surface, even though the strength of distortion gradually decreases with increasing distance between sensor and surface. As a consequence, there is no easy correction formula that would permit the

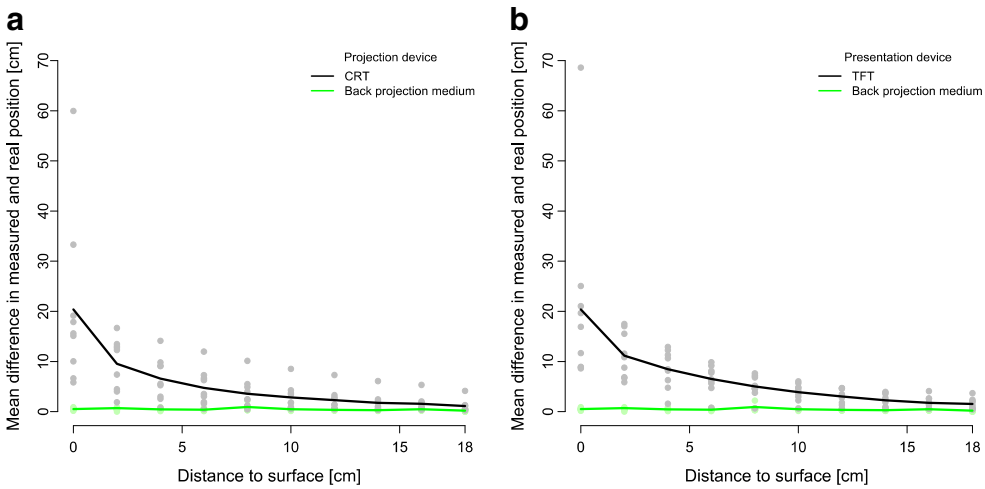

Fig. 2 Mean measurement errors (i.e., the mean Euclidian distance between the measured and the real position) depending on the distance of the sensor to the projection surface for the CRT (**a**) and TFT (**b**) monitors. The electromagnetic devices are depicted in black, the nonelectromagnetic back projection device in green color. The line in saturated color depicts the mean deviation within one *x*/*y* plane. The desaturated points depict the measurement error for each of the nine points within the *x*/*y* plane

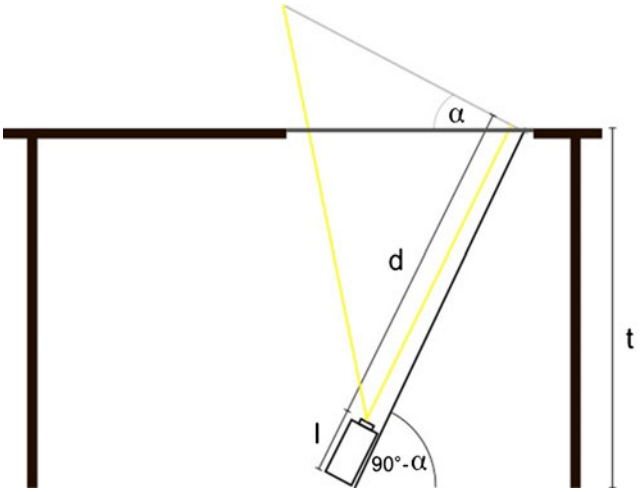

Fig. 3 Sketch of the table setup from side view. *t* denotes the height of the table, *l* the length of the projector, and *d* the distance of the lens to the virtual orthogonal presentation plane. α denotes the angle by which the virtual orthogonal presentation plane is tilted on the presentation medium

distortion to be removed from the measurements by means of some mathematical transformations.

Each data point in Fig. 2 is the mean of 1,000 measurements at the same location. Given that the variance of these 1,000 measurements was extremely small (<0.4 mm), there is no need to calculate statistical tests, because even the 95 % confidence interval would be smaller than the point symbols in the plots. That is, each numerical difference between two data points can be considered a reliable difference.

These data demonstrate that our back projection medium can be used for electromagnetically measuring movement kinematics in close proximity to the display surface, since it is the only device that does not produce any disturbances in the electromagnetic field generated by the tracker system.

Building instructions

The first step when building the experimental table is to choose the correct projector. Most projectors will not be suitable for usage under a table because of the small distance to the projection medium. Thus, the core requirement for the projector is its ability to produce a sharp picture at a range of around 50 cm. These kinds of projectors are usually equipped with a wide-angle lens that allows a good-sized picture to be realized at a short range. The other criterion for picking a projector is its vertical keystone correction capability. Since the projector will project onto the Plexiglas plate from an angle that differs from 90°, it has to be able to correct for it. In our setup, we used a X1230PS (Acer, Inc., Taipeh, Taiwan) projector that meets these criteria. The next step will be to calculate the size of the resulting picture and the table height necessary to achieve it.

The whole setup consists of a table, the fixture of the Plexiglas medium, and the projector ramp (Fig. 3), which should not contain any ferromagnetic material. We used a wooden table, from the surface of which a hole in the dimensions of the Plexiglas medium was cut. In order to fix the medium, a frame made of aluminum was glued to the table, onto which the medium was placed (see Fig. 4). For the tabletop, a simple wooden board is recommended. Since the Plexiglas sheet must be inserted into this board, we need to cut a hole that has exactly the right dimensions. In order to fix the Plexiglas sheet in this hole, we used aluminum rims that were glued to the inside of the hole. A much more elegant solution would be to cut a slightly smaller hole and rim a small frame around it that allows the Plexiglas sheet to be lowered into it. The projector-ramp was built out of wood using three boards yielding a tilted surface on which the projector was fixed. The ramp's tilt must be determined exactly, so that its angle of tilt (α) can be entered directly into the keystone correction.

To obtain a rough estimate of the resulting picture size on the projection medium, it is necessary to calculate the (orthogonal) projection distance. The projector will be projecting on the Plexiglas sheet at an angle α (Fig. 3), determined by the tilt of the projector's ramp. It is advisable to choose a projection angle α around 5° below the maximum keystone correction of which the projector is capable, so as to allow for the correction of construction inaccuracies. The distance of the (virtual) orthogonal projection surface *d* can be calculated as

$$d = \frac{t}{\sin(90^\circ - \alpha)} - l,$$

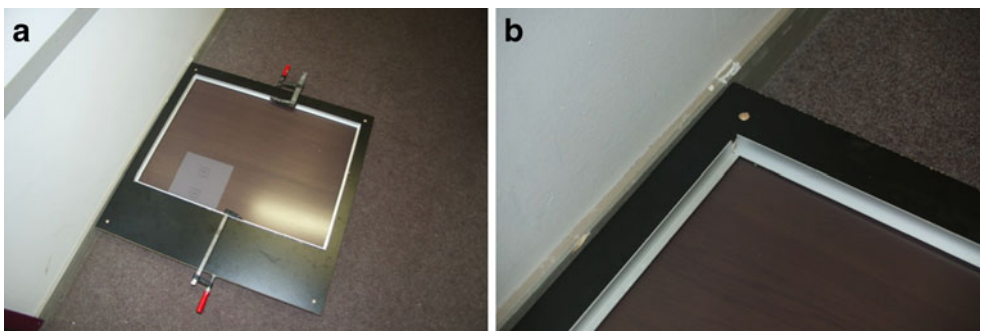

Fig. 4 How the aluminum rim into which the Plexiglas sheet is to be fitted is attached to the table top. **a** Frame. **b** Left upper corner of the frame

where d is the projection distance, t the table height, α the projection angle, and l the projector's length. The projection surface at first is trapezoid because of the nonorthogonal projection surface. The smaller width of this trapezoid can usually be determined by look-up tables provided by the manufacturer (frequently in form of an online tool), depending on the projection distance d. The trapezoid form finally has to be corrected with the projector's keystone projection. Using keystone correction will also result in a reduction of the projection's width. For the projector model we used, the picture width was reduced by approximately 1.15 % per degree of tilt (α).

Conclusion

The setup presented here allows electromagnetic motion capture systems (such as Polhemus) to be used with computer-generated visual stimuli without distortions of the sensor signals that would be caused by electromagnetic presentation media. Using this simple setup makes it possible to present simple geometrical shapes, photos of faces or natural scenes, and even movies while recording the kinematics of trajectories for reaching and pointing movements.

Appendix

Numeric measurement errors between measured and real positions for each tested location and projection device

Table 1 Measurement errors (in centimeters) for the CRT presentation device and all distances to the projection surface (0–18 cm) and for all nine positions in the *x*/*y* plane parallel to the projection surface

Distance	*x*/*y* Position								
	1	2	3	4	5	6	7	8	9
18	0.381	1.301	1.077	0.262	0.327	4.132	0.599	0.570	1.173
16	0.809	2.028	1.793	0.482	0.372	5.323	1.003	0.638	1.554
14	0.881	2.435	2.171	0.499	0.414	6.085	1.041	0.367	1.829
12	1.350	3.280	2.816	0.731	0.615	7.298	1.393	0.466	2.605
10	1.796	4.259	3.668	0.849	0.831	8.513	1.733	0.499	3.381
8	2.473	5.485	4.880	1.167	1.176	10.108	2.389	0.460	3.976
6	3.506	7.274	6.630	1.597	1.893	11.964	3.037	0.502	6.274
4	5.258	9.809	9.125	2.544	2.990	14.109	5.531	0.781	9.058
2	7.377	12.726	12.282	4.015	4.450	16.665	13.454	1.863	13.011
0	10.031	15.595	15.103	5.833	6.641	19.131	33.299	59.955	17.869

Table 2 Measurement errors (in centimeters) for the TFT presentation device and all distances to the projection surface (0–18 cm) and for all nine positions in the *x*/*y* plane parallel to the projection surface

Distance	*x*/*y* Position								
	1	2	3	4	5	6	7	8	9
18	0.896	2.346	2.097	0.504	0.427	3.674	1.281	0.596	1.865
16	1.347	2.583	2.628	0.645	0.552	4.074	1.509	0.597	1.818
14	2.279	3.799	3.530	0.873	0.905	3.927	1.837	0.485	2.728
12	3.263	4.646	4.703	1.294	1.790	4.580	2.759	0.558	3.468
10	4.834	5.659	6.036	2.223	2.938	4.693	3.513	0.586	4.188
8	7.178	6.813	7.631	3.755	5.139	4.708	4.559	0.636	4.580
6	9.847	7.746	9.164	6.447	8.103	4.709	6.086	0.771	5.629
4	12.890	8.435	10.615	11.270	12.242	4.766	8.173	1.567	6.273
2	15.521	8.778	11.547	17.475	17.034	5.856	10.829	6.690	6.844
0	16.902	8.833	11.661	68.620	19.643	8.928	20.389	25.046	8.607

Table 3 Measurement errors (in centimeters) for our back projection medium presentation device and all distances to the projection surface (0–18 cm) and for all nine positions in the *x*/*y* plane parallel to the projection surface

Distance	*x*/*y* Position								
	1	2	3	4	5	6	7	8	9
18	0.169	0.270	0.222	0.327	0.300	0.529	0.223	0.497	0.118
16	0.222	0.280	0.251	0.342	0.275	0.615	0.312	0.508	0.176
14	0.358	0.351	0.367	0.493	0.467	0.705	0.375	0.570	0.134
12	0.290	0.320	0.935	0.452	0.730	0.630	0.407	0.261	2.188
10	0.302	0.288	0.417	0.457	0.314	0.735	0.518	0.290	0.081
8	0.332	0.291	0.471	0.458	0.337	0.864	0.608	0.366	0.090
6	0.368	0.375	0.682	0.551	0.414	0.871	0.657	0.476	0.000
4	0.414	0.463	0.539	0.520	0.404	0.870	0.689	0.450	0.149
2	0.169	0.270	0.222	0.327	0.300	0.529	0.223	0.497	0.118
0	0.222	0.280	0.251	0.342	0.275	0.615	0.312	0.508	0.176

References

Baldauf, D., & Deubel, H. (2008). Visual attention during the preparation of bimanual movements. *Vision Research, 48*(4), 549–563. doi:10.1016/j.visres.2007.11.023

Basile, B. M., & Hampton, R. R. (2011). Monkeys recall and reproduce simple shapes from memory. *Current Biology: CB, 21*(9), 774–778. doi:10.1016/j.cub.2011.03.044

Diedrichsen, J., Ivry, R. B., Hazeltine, E., Kennerley, S., & Cohen, A. (2003). Bimanual interference associated with the selection of target locations. *Journal of Experimental Psychology. Human Perception and Performance, 29*(1), 64–77.

Ernst, M. O. (2007). Learning to integrate arbitrary signals from vision and touch. *Journal of Vision*, *7*(5), 7 1–14. doi: 10.1167/7.5.7

Ghahramani, Z., Wolpert, D. M., & Jordan, M. I. (1996). Generalization to local remappings of the visuomotor coordinate transformation. *The Journal of Neuroscience, 16*(21), 7085–7096.

Hommel, B. (2004). Event files: Feature binding in and across perception and action. *Trends in Cognitive Sciences, 8*(11), 494–500. doi:10.1016/j.tics.2004.08.007

Jonikaitis, D., & Deubel, H. (2011). Independent allocation of attention to eye and hand targets in coordinated eye-hand movements. *Psychological Science, 22*(3), 339–347. doi:10.1177/0956797610397666

Körding, K. P., & Wolpert, D. M. (2006). Bayesian decision theory in sensorimotor control. *Trends in Cognitive Sciences, 10*(7), 319–326. doi:10.1016/j.tics.2006.05.003

Prinz, W. (1984). Modes of linkage between perception and action. In W. Prinz & A.-F. Sanders (Eds.), *Cognition and motor processes* (pp. 185–193). Berlin: Springer.

Prinz, W. (1997). Perception and action planning. *European Journal of Cognitive Psychology, 9*(2), 129–154.

Song, J.-H., Takahashi, N., & McPeek, R. M. (2008). Target selection for visually guided reaching in macaque. *Journal of Neurophysiology, 99*(1), 14–24. doi:10.1152/jn.01106.2007

Striemer, C. L., Chapman, C. S., & Goodale, M. A. (2009). "Real-time" obstacle avoidance in the absence of primary visual cortex. *Proceedings of the National Academy of Sciences of the United States of America, 106*(37), 15996–16001. doi:10.1073/pnas.0905549106

Todorov, E. (2009). Efficient computation of optimal actions. *Proceedings of the National Academy of Sciences of the United States of America, 106*(28), 11478–11483. doi:10.1073/pnas.0710743106

Zehetleitner, M., Hegenloh, M., & Müller, H. J. (2011). Visually guided pointing movements are driven by the salience map. *Journal of Vision, 11*(1), 1–18.